nature portfolio

Peer Review File

A region-confined PROTAC nanoplatform for spatiotemporally tunable protein degradation and enhanced cancer therapy

REVIEWER COMMENTS

Reviewer #1 (PDT, nanomedicine):

The submitted paper reports an extensive investigation of an extremely elaborated PROTAC design, featuring a region-confined PROTAC nanoplatform that integrates both reactive oxygen species (ROS)-activatable and hypoxia-responsive PROTAC prodrug for BRD4 targeting. Thus, numerous in vitro and in vivo studies are performed to show that PROTAC nanoparticles are effectively degrading BRD4 across both normorxia and hypoxia areas, markedly hindering tumor progression in breast and head-neck cancer models. While the design concept is very ambitious, I find the attempt to target the PRTOAC-nanoparticles to the tumour site via the EPR questionable, particularly considering that in patients this type of passive targeting is highly not effective due to the great tumour heterogeneity. Therefore, although this study tries to address both cancerous cells and CSC, the actual demonstration of the BRD4 degradation pathways in the CSC type has not been achieved. Only indirect evidence and possibly interferences with the PDT activity have been shown. Thus, the scheme reported in Figure 1b is purely speculative at this stage. Overall, I found the manuscript very difficult to read, due to the mixing of experimental evidences and hypothesis to still be demonstrated. Certain Figures are also unreadable (e.g. Fig 5) due to the reduced size of the images. Overall, I recommend the paper for publication only after the authors will have revised their statements and adopt a less speculative approach to the description of their results.

Reviewer #2 (PROTAC, cancer therapy):

This article by Gao et al describes the development of nanoparticles targeting different cancer cells and responding to different cues to improve their efficiency. The nanoparticles also carry a PROTAC cargo used as a cytotoxic payload. This work aims to overcome some of the limitations of PROTAC molecules, namely pharmacokinetics and to improve tumor specificity. Overall, the manuscript is of decent quality and all the authors' claims are very clearly supported by experiments, to the extent that it almost overwhelms the reader. The amount of work put into this paper is outstanding. This reviewer wonders if all experiments were necessary and if they need to be included in the main text or could be moved to the supporting section. This would allow to highlight the main experiments and streamline the findings. The writing of the manuscript needs some improvement to make the article clearer and give it a better flow. The article would benefit to be made easier to understand. Since the article contains numerous abbreviations and acronyms, it would be good to include in the supporting information a list of all the acronyms/abbreviations used throughout the paper.

In this paper, the authors develop a nanoparticle platform responsive to different extra or intracellular stimuli. Tumor specific accumulation is achieved by using an MMP2 cleavable linker,

leading to dePEGylation of the nanoparticles, their cellular uptake and breakdown in the acidic endosomal environment. In addition, the PROTAC payload is cleaved from the polymer by reactive oxygen species generated by laser irradiation of a photosensitizer. To specifically target stem-like cancer cells, the authors synthesized a redox sensitive PROTAC prodrug. The association of all these technologies creates a very complex platform that the authors characterize very well, from the size of the nanoparticles to the release of the PROTAC in response to different cues. Using this platform the authors claim to have overcome most of PROTACs limitations but have introduced major limitations on their own. Photodynamic therapy involves light laser irradiation at the tumor site, which involves surgery for some solid tumors. This reviewer wonders if an acid cleavable linker responding to tumor specific uptake would be efficient in both regular and stem-like cancer cells.

Given the amount of work and the care given to characterizing their platform, this paper has the potential to interest the readers of Nature Communications. However, it needs to go through some revisions before being published.

• The grammar and the spelling of the paper and the supporting information needs to be thoroughly checked and modified. As it stands, the paper is too confusing and errors or complex sentences take the attention away from the results. Special attention needs to be brought to the Abstract, the introduction, and the conclusion. This will elevate the quality of the manuscript tremendously and will make it easier to follow. Some examples below:

o Line 46: and penetrate into deep tumor via liable to MMP2. A word seems to be missing.

o Line 67: PROTAC is misspelled

o Line 103: we further innovated a hypoxia-responsive PROTAC

o Line 676: we engineered fashioned a region-confined PROTAC

• The PGDAT nanoparticles were synthesized using a ratio of 2/1 PROTAC monomer to photo sensitizer monomer. Did the authors try different ratios of PROTAC/Photosensitizer (PPa)? Was the 2/1 ratio the one giving the best results?

• Figure 2c. and figure 2e. The BRD4 levels in figure 2c appear much higher than in figure 2e, or at least the corresponding band on the western blot appears more important. Is this due to overexposure to try to really highlight the degradation of BRD4 at 500 nM ARV771? Or is the level of BRD4 lower in the cells treated with ARV771-TK?

• Figure 3b/e + 8c. the microscopy images are hard to read in printed version and sometimes still very hard to read on a computer screen. It is extremely unclear to an untrained eye to see major differences. These figures would benefit from being moved to the supporting information and being much larger. For all the cell imaging, it would be interesting to add in the supporting information a phase contrast image of the cells.

• Figure 3e. Was the cytotoxicity of the irradiation tested? Would that be a concern?

• Figure 8a: Levels of HIF also appear much weaker with PGDAT@N than for other nanoparticles or the PBS control. Is HIF expression or stability being impacted by PGDAT@N?

• Figure 8c. The overlay between the two colors used for pimo and Cyanine are extremely hard to tell apart. It would be good to mention in the caption what each smaller zoomed in section corresponds to. I suppose, the top one is an overlay while the two bottom ones correspond respectively to Pimo and Cy.

• In general, comparing the in vivo efficacy of PDGAT versus PDGAT@N. What would be the impact of restarting the treatment with PDGAT for the mice that relapsed? Do the authors expect PDGAT@N to still outperform PDGAT? I understand that performing this experiment would be asking a lot and would not necessarily add much to the paper. This is more sheer curiosity.

• Supplementary figure 25: Title of the caption needs to be changed to Heat map.

• Supplemetary figure 51 + 52: The overall quality of the analysis of compound 32 is very poor. The resolution of the NMR spectrum does not allow for a good assignment of the signals. The MS spectrum needs to be shown in full and not zoomed in. This mas spectrum cannot be used to interpret the purity of this compound. The characterization of this compound needs to be brought to the same level of detail as the previous compounds in this paper.

Reviewer #3 (CSC, cancer therapy):

Gao and coauthors are dealing with an important problem of targeting tumor heterogeneity using PROTAC-based treatment. The authors proposed an elegant design of the BRD4-specific, ROS- and hypoxia-activated PROTAC nanoplatform.

Overall, this interesting and comprehensive study can undoubtedly be of interest to the interdisciplinary scientific community. The results shown in this manuscript are novel and pertinent. Still, some issues must be clarified.

Main concerns:

1. Clinical relevance:

- The activation of the PROTAC system is pH dependent and is responsive to low intracellular acidity (pH 5.5-6.5). However, some tumor types upregulate expression of Na+/H+ exchanger 9 (NHE9) associated with more alkaline endosomes (pH > 6.5), stemness, and worse clinical outcome (e.g., Kondapalli et al., Nat. Commun. 2015; Ko et al., PNAS Nexus 2022). NHE9 is upregulated in different malignancies, and its high expression is related to poor prognosis (e.g., in CRC and ESCC).

- Next, the problem with targeting BRD4 could be associated with potential target escape due to tumor cell plasticity and heterogeneity, including CSCs. One suggested approach could be a dual/multiple targeting, leading to a synergistic effect and preventing tumor cell escape.

- Next, the tissue penetration depth of the laser irradiation is limited to a few mm, sufficient to see a therapeutic effect in subcutaneous tumor models but not for orthotopic tumors / in a clinical setting.

- Together, these considerations raise concern about the possible clinical applicability of the suggested PROTAC nanoplatforms.

2. In vivo models:

- The authors described MDA-MB-231 and HN30 orthotopic murine models in the material and methods; however, the results included in the figures were obtained only with subcutaneous models. Validation of the therapeutic effect in the orthotropic models would increase the translational potential of the described nano platform. The authors are encouraged to include these models in the revised study.

- The group size (n = 6) and partially overlapping tumor growth curves (e.g., for PGDA+Laser vs. PGDAT+Laser in Figure 5D) raise a concern about statistical analysis, giving p = 0.0084 for the mentioned groups. The authors should clarify the statistical method in the legends of Figure 5.

3. Other concerns:

- Figure 5-7: how is it possible that PGDAT + Laser treatment leads to an increase in the hypoxic area and CSC populations?

- Although the authors conclude that BRD4 degradation influences the CSC population, the evidence from in vivo experiments e.g., analysis of the CSC populations in the experimental treated tumors, did not confirm this statement. The results of the flow cytometry examination of CD44+/CD24- cells did not show a statistically significant difference between control PBS-treated and PGDAT@N + Laser treated mice.

Response to the Editor and Reviewers

We sincerely thank the editor and reviewers for taking time to review the manuscript and for the constructive feedback. In response to the suggestions provided, we have comprehensively revised our manuscript. Specifically, we have: 1) simplified the main text and moved some figures and data into Supplementary Information in the revised manuscript; 2) made a point-to-point response to all the technical questions and concerns of all the reviewers; 3) explained the advantage of the PROTAC NPs for tumor targeting and BRD4 degradation pathway in cancer stem-like cells.

Reviewer #1 (PDT, nanomedicine):

The submitted paper reports an extensive investigation of an extremely elaborated PROTAC design, featuring a region-confined PROTAC nanoplatform that integrates both reactive oxygen species (ROS)-activatable and hypoxia-responsive PROTAC prodrug for BRD4 targeting. Thus, numerous in vitro and in vivo studies are performed to show that PROTAC nanoparticles are effectively degrading BRD4 across both normorxia and hypoxia areas, markedly hindering tumor progression in breast and head-neck cancer models. While the design concept is very ambitious, I find the attempt to target the PRTOAC-nanoparticles to the tumour site via the EPR questionable, particularly considering that in patients this type of passive targeting is highly not effective due to the great tumour heterogeneity. Therefore, although this study tries to address both cancerous cells and CSC, the demonstration of the BRD4 degradation pathways in the CSC type has not been achieved. Indirect evidence and possibly interferences with the PDT activity have been shown. Thus, the scheme reported in Figure 1b is purely speculative at this stage. Overall, I recommend the paper for publication after the authors will have revised their statements and adopt a less speculative approach to the description of their results.

Response: We appreciate the insightful comments of the reviewer. We had carefully revised the manuscript and adapted all the statement more moderate and convenience than the previous version. All revision were highlighted in the revised main manuscript.

1. We completely agree with the reviewer that tumor heterogeneity is one of the major challenges for nanoparticle-based therapeutic delivery and cancer therapy. To address this concern, apart from the EPR effect of nanomedicine, an extracellular matrix metalloproteinase (MMP-2)-triggered dePEGylation strategy was employed in this study to improve tumor accumulation and penetration of the nanoparticles. The MMP-2-responsive PROTAC nanoparticles displayed dramatically improved tumor distribution and penetration in tumor mass. Bioinformatics analysis of the clinical database further validated that MMP-2 is overexpressed in a broad spectrum of solid tumors in human patients, which can serve as a general stimulus to induce dePEGylation of the PROTAC nanoparticles and facilitate their accumulation at the tumor site, thus overcome tumor heterogeneity.

To further combat tumor heterogeneity and promote nanoparticle distribution at the tumor site, we will exploit other kinds of stimulus in future study. For example, fibroblast activation protein-α (FAP), which is up-regulated in various solid tumors, therefore are promising for increasing tumor accumulation of nanomedicine **(Supplementary Fig. 71)**.

We added above discussion in page 36 of the revised manuscript.

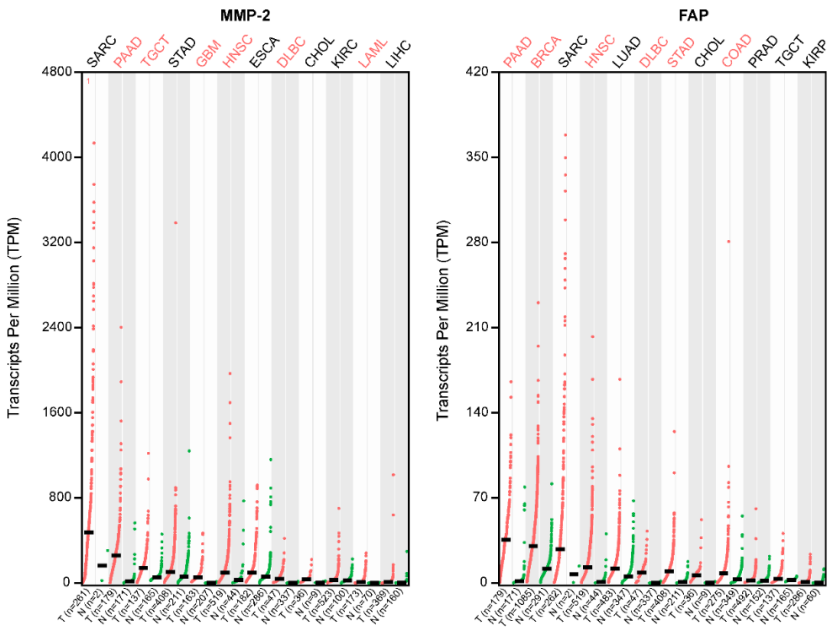

Supplementary Fig. 71. The MMP-2 and FAP gene expression profiles in the different tumor types and normal tissue of human patients (http://gepia.cancer-pku.cn/).

2. To validate hypoxia-liable PROTAC prodrug-mediated regulation of cancer stem-like cell (CSC) signaling pathway demonstrated in Figure 1b, and elucidate the interference of PDT, we had performed RNA-seq analysis, q-PCR assay and western blot examination to investigate how BRD4-degradation affected CSC proliferation and suppressed tumor growth.

In cell culture level, RNA-seq analysis displayed that ARV771-treatment significantly downregulated the crucial genes regulating cell proliferation in CSCs, including murine double minute 2 (MDM2), cyclin-dependent kinase 4 (CDK4), cyclin-dependent kinase 7 (CDK7), cyclin-dependent kinase 1 (CDK1), cyclin-dependent kinase 6 (CDK6) and so on. Noticeably, several oncogenes (e.g., kirsten rat sarcoma viral oncogene (KRAS), c-Mesenchymal-epithelial transition factor (MET), Abelson murine leukemia viral oncogene homolog 1 (ABL1), and murine leukemia viral oncogene homolog 1 (RAF1)) were downregulated as well **(Figure 5f)**.

Differentially expressed genes (DEGs) analysis revealed that BRD4-degradation induced dramatic upsurge in cell apoptosis-related gene (e.g., tumor necrosis factor (TNF) receptor family and cyclin dependent kinase inhibitor 1A (CDKN1A)) in both MDA-MB-231 CSCs and normal tumor cells **(Supplementary Fig. 33)**. In contrast, several stemness-related genes were downregulated in ARV771-treated CSCs (e.g., wingless-type MMTV integration site family member 7B (WNT 7B), Rap1 interacting factor 1 (RIF1), Kruppel like factor 4 (KLF4), SRY-Box transcription factor 4 (SOX4) and cell division cycle 73 (CDC73)) **(Figure 5g).**

Quantitative polymerase chain reaction (qPCR) analysis further confirmed the changes in the expression levels of crucial genes after CSCs were treated with ARV771. For instance, the expression of MDM2, CDK4 and CDK6, which are essential for cell proliferation, was obviously inhibited by 5.5-, 5.0- and 2.7-fold, respectively, compared with that in the PBS group when CSCs were treated with ARV771. Concurrently, the level of CDKN1A (corresponding to the p21 protein), which can inhibit the function of CDK4 and CDK6, was increased 65.6-fold compared to that in the PBS group after CSCs were treated with ARV771 **(Figure 5h)**. In addition, the expression of stemness-related genes (e.g., WNT 7B, SOX4, KLF4, RIF1, and CDC73) decreased compared to

that in the PBS group after CSCs were subjected to ARV771 treatment **(Figure 5i).**

Next, western blot analysis revealed significant BRD4 degradation in a dose-dependent manner for both ARV771 and ARV771-Nb, which had DC_{50} values of 73 nM and 95 nM respectively, which subsequently downregulated CDK4/6 and upregulated p21 **(Figure 6c, d, Supplementary Fig. 46a, b)**. In contrast, the hypoxia-inert control, ARV771-Ph, had negligible effects on the expression of these proteins **(Figure 6e, Supplementary Fig. 46c)**. CDK4/6 and p21 are all critical regulators of apoptosis pathway. Therefore, it could be concluded that BRD4 degradation induced apoptosis of CSCs.

Moreover, ARV771 and ARV771-Nb impaired the ability of CSCs to form tumor spheroids, as evidenced by marked decreases in the number of tumor spheroids after 12 days of treatment with ARV771 and ARV771-Nb**.** For instance, there were approximately 90% and 83% fewer tumor spheroids after treatment with 1.0 μM ARV771 and 1.0 μM ARV771-Nb, respectively. In contrast, hypoxia-insensitive ARV771-Ph exhibited no significant difference (p = 0.1515) in the number of tumor spheroids compared to that in the PBS control group at different concentrations **(Figure 6f)**. Taken together, these data confirmed that ARV771-Nb could be activated within CSCs and selectively combat CSCs through its ability to induce BRD4 degradation.

Furthermore, western blot analysis confirmed notable BRD4 degradation in the PGDAT + laser group, with a 65% inhibition rate, and in the PGDAT@N + laser group, with 80% degradation, and BRD4 removal inhibited CDK4 and CDK6 expression while upregulating the expression of p21 **(Figure 6n, Supplementary Fig. 54)**. Upregulated p21 can further inhibit the activities of the CDK4 and CDK6 proteins, leading to the upregulation of cleaved caspase 3, which promotes tumor cell apoptosis.

The preeminent performance of PGDAT@N + laser in preventing tumor recurrence prompted a deeper exploration of its underlying mechanisms. Flow cytometry analysis revealed a significant decrease in the percentage of CSCs in the PGDAT@N + laser group compared to that in the PBS group (P value of 0.0039, **Figure 6o**), which was mostly attributed to the effective inhibition of CSCs by hypoxia-activated ARV771-Nb. These results were further supported by the downregulated expression of key CSC

markers in the PGDAT@N + laser group (e.g., Nanog, Oct4 and Sox2) **(Supplementary Figs. 55, 56)**.

Overall, above data collectively validated that BRD4 degradation inhibited both the normal tumor cells and the stem-like cancer cells *in vitro* and *in vivo*, therefore, the hybrid PGDAT@N PROTAC nanoparticles hold promising potential for ablating the whole breast tumor by overcoming tumor heterogenicity.

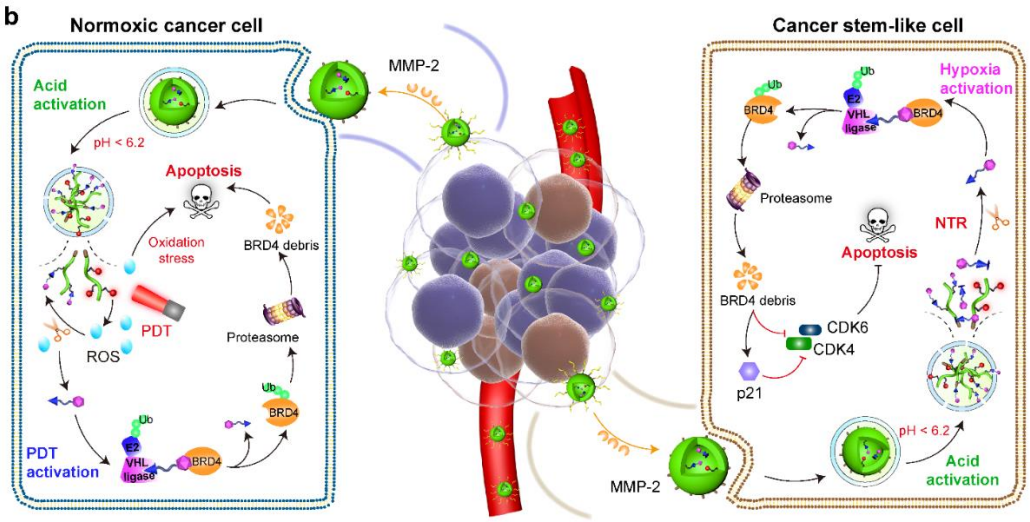

Figure 1b, Cartoon illustration of the PGDAT@N nanoparticle eliminates tumor cells in normoxic and hypoxic areas simultaneously by self-complementary degrading BRD4 protein. PGDAT@N nanoparticle reaches tumor tissue after i.v. injection via MMP-2-induced dePEGylation, which enhances nanoparticles accumulation and penetration at the tumor site. After internalized into tumor cells, the PROTAC nanoparticle recovers its photoactivity due to protonation of the DPA groups and dissociation of the nanoparticle. The effluent ROS is then generated in the normoxic region under laser irradiation to release ARV771 via cleaving the TK linkage. The combination of BRD4 degradation and PDT cumulatively induce apoptosis of the normoxia tumor cells. Meanwhile, upon internalization by hypoxia cancer cells, hypoxia-activatable PROTAC derivate is divulged from the dissociated PGDAT@N nanoparticles, and then restored ARV771-Nb prodrug to parental PROTAC with nitroreductase (NTR) for sweeping cancer stem-like cells (CSCs). BRD4 degradation downregulates cell cycle proteins including cyclin-dependent kinase 4 (CDK4) and cyclin-dependent kinase 6 (CDK6), meanwhile upregulates cyclin-dependent kinase inhibitor 1A (p21) to induce hypoxia cancer cell apoptosis. The obliteration of both normoxic and hypoxic tumor cells with the region-confined PROTAC nanoplatform enable tumor regression efficiently.

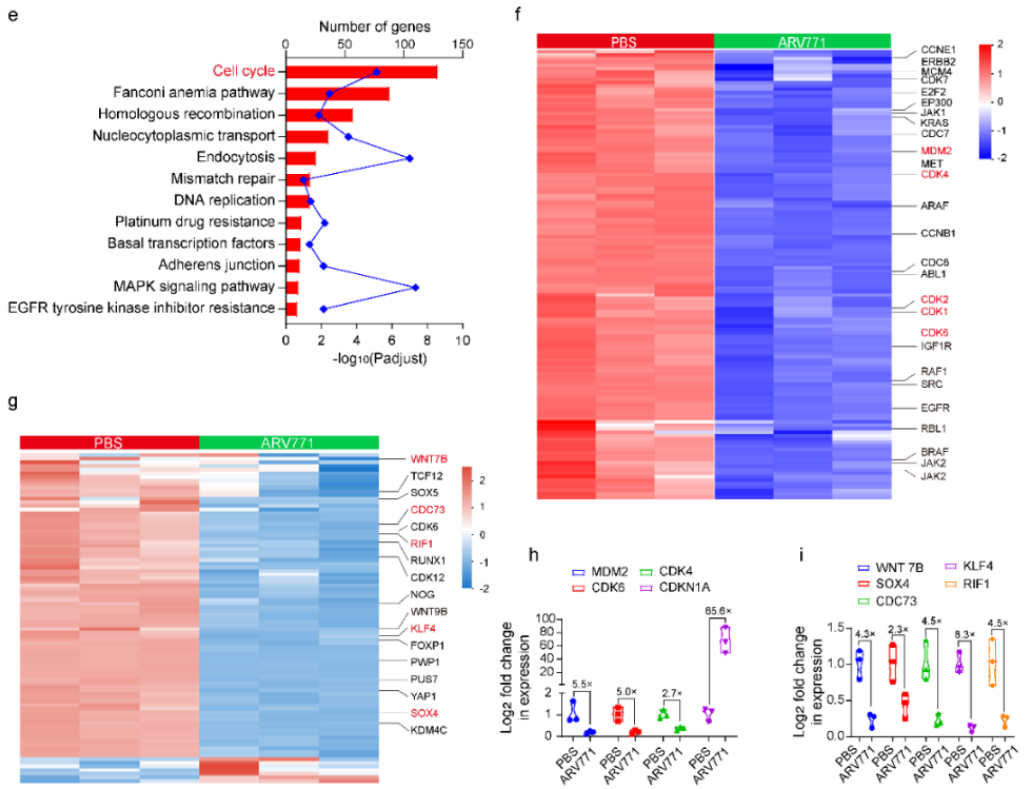

Figure 5e-g, RNA-seq analysis of differential expression genes between MDA-MB-231 stem-like cells treated with PBS or ARV771 at the concentration of 1.0 μM for 24 h. **e,** KEGG enrichment histogram of differentially expressed genes (statistical difference was calculated using Fishers exact test, n = 3 biologically independent cells). **f,** heatmap of differentially expressed genes associated with cell cycle and **(g)** cell stemness (n = 3 biologically independent cells, red and blue colors represent upregulated or downregulated genes respectively). **h & i,** Quantitative PCR assay of the (**h**) cell cycle- and (**i**) cell stemness-related mRNA levels in MDA-MB-231 CSCs post 24 h incubation with 1.0 μM of ARV771 (n = 3 biologically independent cells).

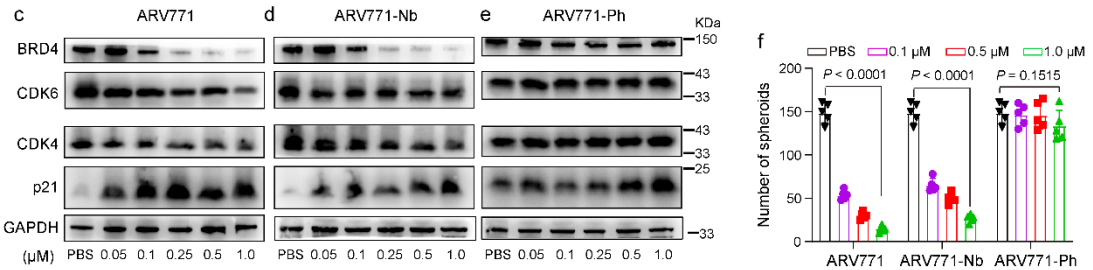

Figure 6c-e, Western blot assay of BRD4 expression and its downstream protein of CDK4, CDK6 and p21 in MDA-MB-231 stem-like cells with **(c)** ARV771, **(d)** ARV771-Nb and **(e)** ARV771-Ph treatment for 24 h. **f,** Number of the formed tumor spheroids (diameter > 50 μm) after the MDA-

MB-231 cells with various treatments for 12 days (n = 5 biologically independent cells). Statistical analysis was performed by two-sided unpaired t-test.

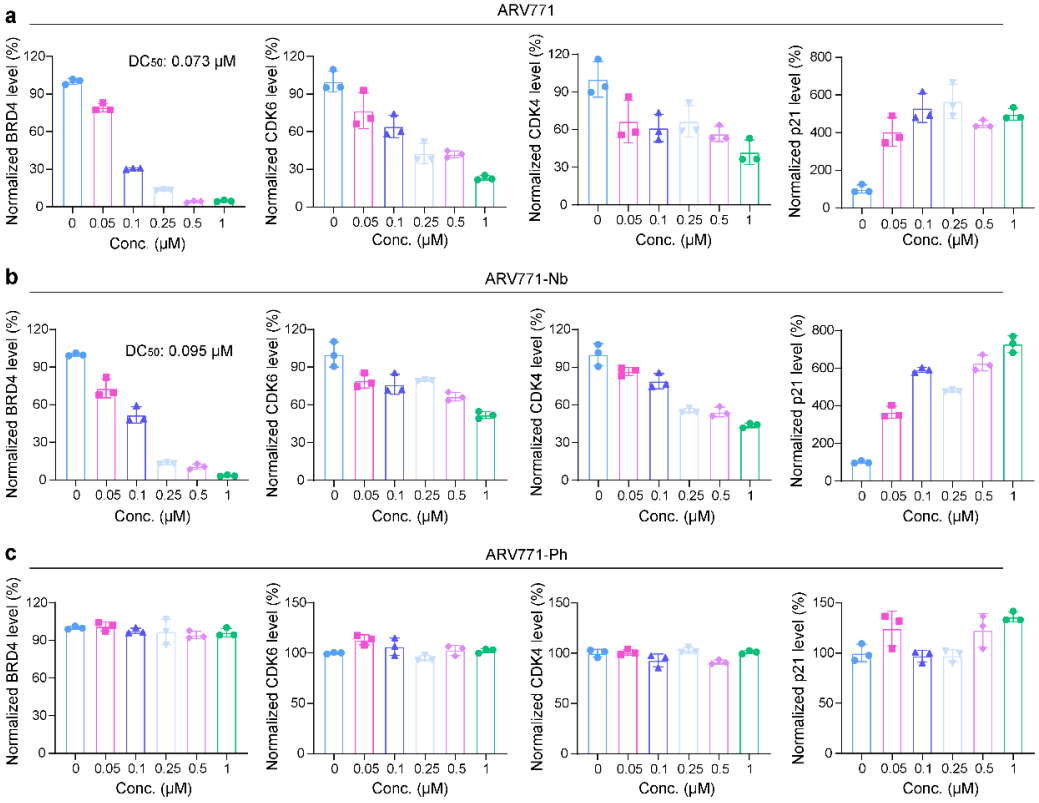

Supplementary Figure 46. Semi-quantitation of the western blot band of MDA-MB-231 stem-like cells after being treated with (**a**) ARV771, (**b**)ARV771-Nb and (**c**) ARV771-Ph for 24 h (n = 3 biologically independent cells). All data are presented as mean ± SD.

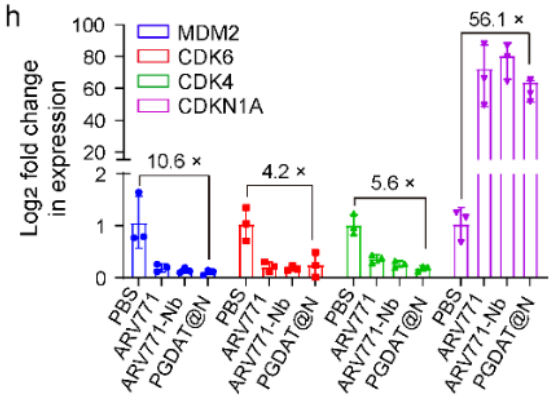

Figure 6h, Quantitative PCR detection of mRNA expression post 24 h treatment with different formulations in MDA-MB-231 stem-like cells (n = 3 biologically independent cells).

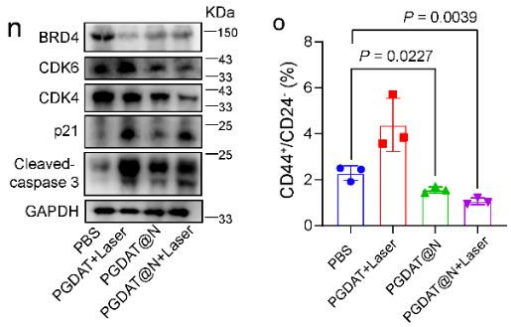

Figure 6n, Western blot assay of PROTAC nanoparticle induced BRD4 degradation and differential expression of its downstream proteins. **o**, Flow cytometry examination of CSCs percentage in the tumor tissue post different treatments (n = 3 biologically independent mice). Statistical analysis was performed by two-side unpaired t-test.

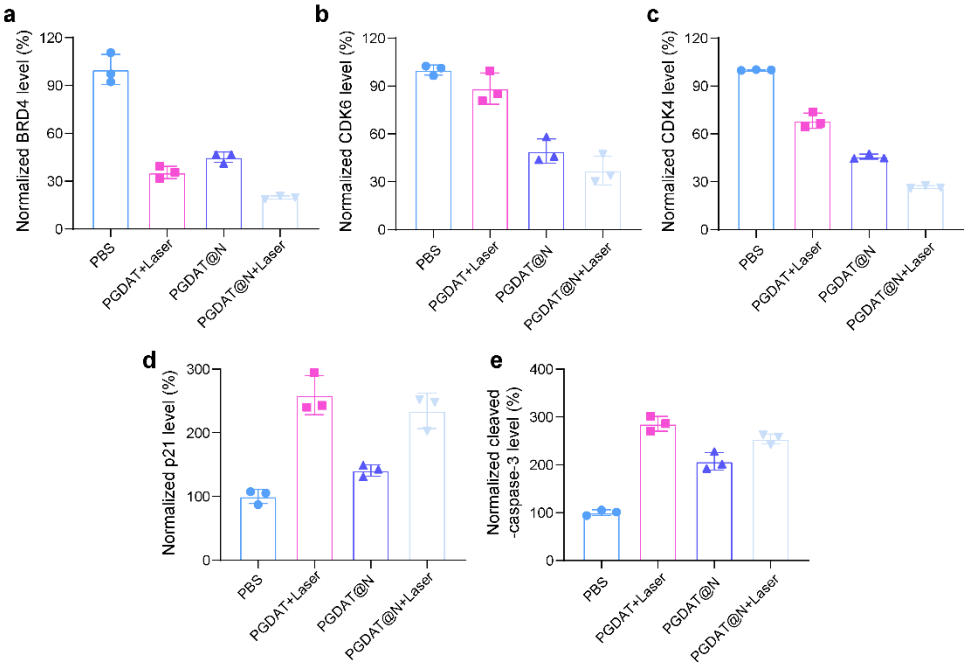

Supplementary Figure 54. Semi-quantitation of the western blot band of different protein (**a**) BRD4, (**b**) CDK6, (**c**) CDK4, **(d)** p21 and **(e)** cleaved-caspase-3 in the tumor tissues after the MDA-MB-231 tumor-bearing mice were treated with various methods (n = 3 biologically independent mice). All data are presented as mean ± SD.

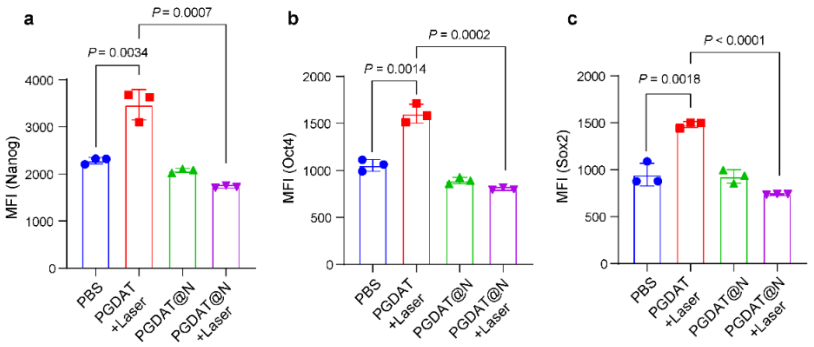

Supplementary Figure 55. Flow cytometric assay of intratumoral (**a**) Nanog, (**b**) Oct4 and (**c**) Sox2 expression after the tumor-bearing mice subjected to predetermined treatments (n = 3 biologically independent mice). Statistical analysis was performance by two-sided unpaired t-test. All data are presented as mean ± SD.

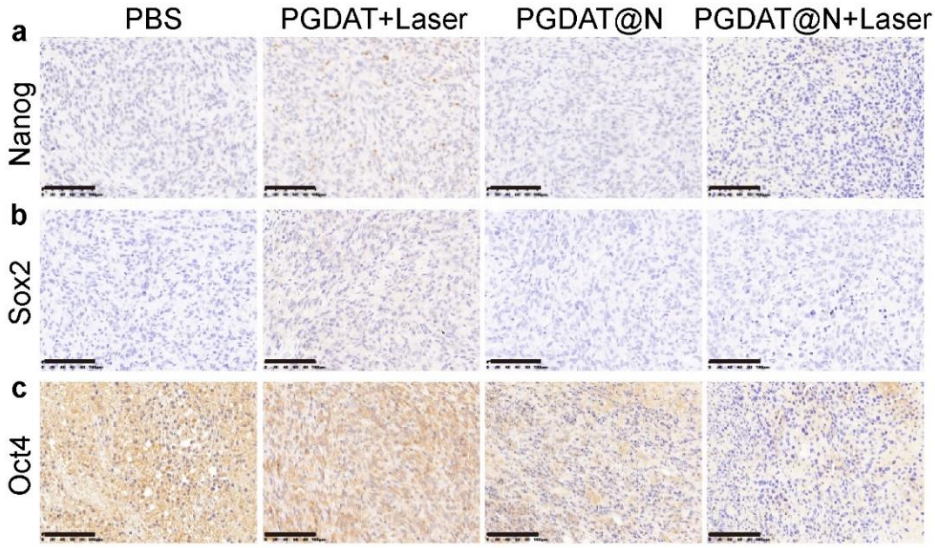

Supplementary Figure 56. IHC examination of (**a**) Nanog, (**b**) Sox2 and (**c**) Oct4 expression in the tumor sections post the predetermined treatments (scale bar = 100 μm).

3. To improve readability of the manuscript as suggested by the reviewer, we reorganized the structure of the manuscript to firstly present the scientific hypothesis, and then discuss the data collected. Furthermore, we thoroughly revised the manuscript with the assistance of professional editors from Nature Research Editing. The editing certificate was attached at the end of this response letter.

4. To highlight the key points of the manuscript, we moved part of the data from the

main manuscript to the Supplementary Information (listed below), and amplified the microscopic images into full size as list below:

Original Figure number	Updated Figure numbers in the revised manuscript
Figure 2d and Figure 2f	Supplementary Figure 8
Figure 2h	Supplementary Figure 20
Figure 2l and Figure 2m	Supplementary Figure 22
Figure 3b	Supplementary Figure 23
Figure 3e	Supplementary Figure 24
Figure 5e	Supplementary Figure 27
Figure 7c	Supplementary Figure 45
Figure 7i	Supplementary Figure 48
Figure 7k	Supplementary Figure 51
Figure 7o	Supplementary Figure 52

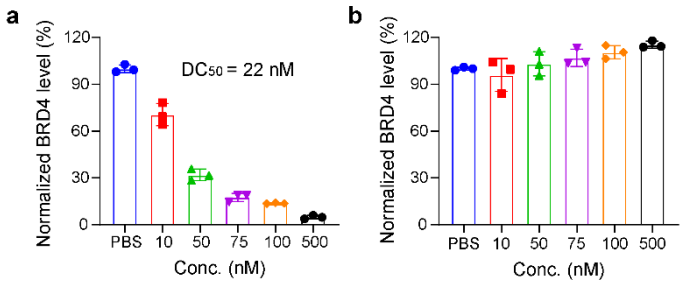

Supplementary Figure 8. Normalized BRD4 expression in MDA-MB-231 cells with the treatment of (a) ARV771, (b) ARV771-TK. All data are presented as mean ± SD. (n = 3 biologically independent cells).

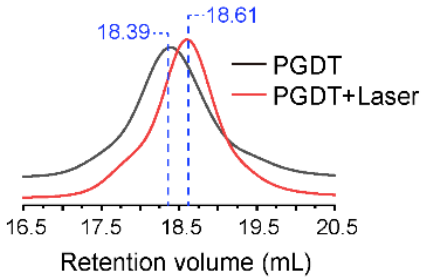

Supplementary Figure 20. The representative GPC plots of PDT-induced molecular weight change of PGDT polymer.

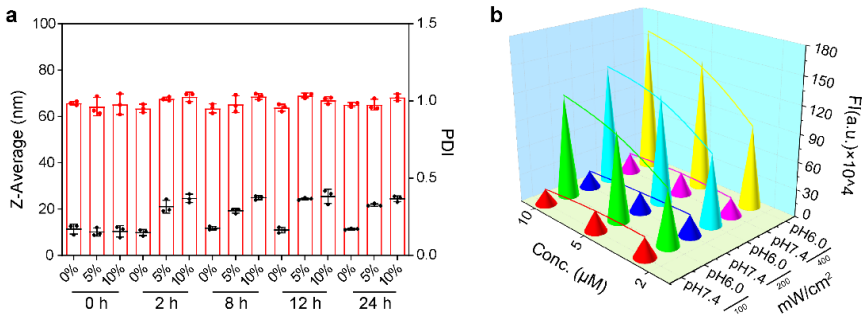

Supplementary Figure 22. a, Averaged hydrodynamic diameter and PDI of PGDAT nanoparticle as a function of FBS concentrations and incubation time (n = 3 independent experiments). **b,** ROS generation property of PGDAT nanoparticle with different dosages and photo-density at the neutral pH 7.4 and acidic pH 6.0 condition. SOSG probe was added into the PGDAT nanoparticle suspensions before laser irradiation and the fluorescence intensity was detected immediately post laser treatment.

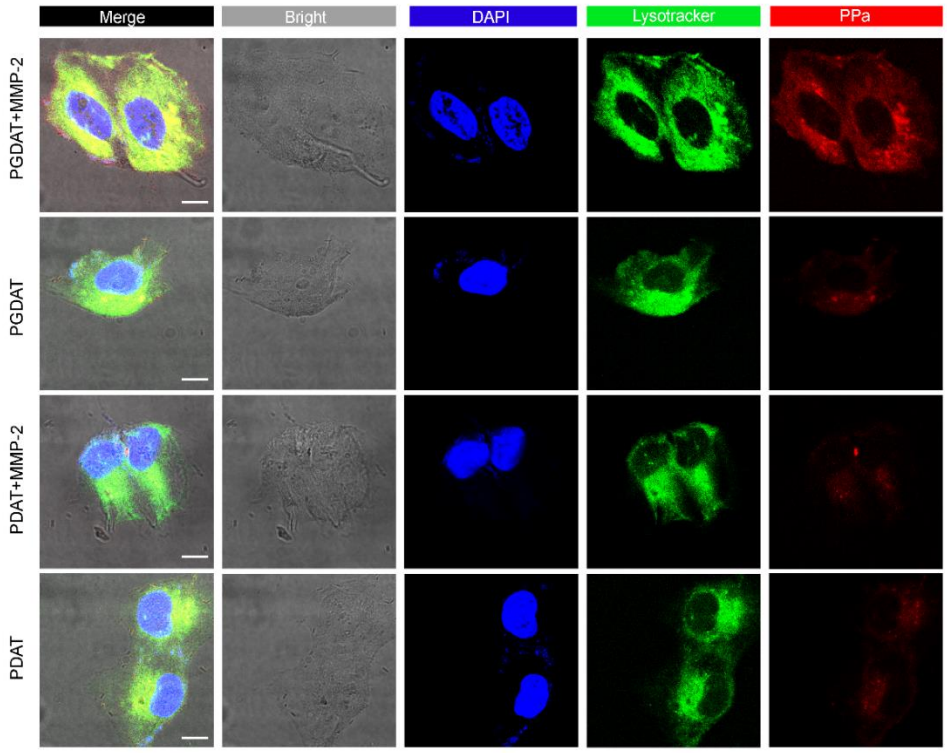

Supplementary Figure 23. Representative CLSM images of the intracellular distribution of the PROTAC nanoparticle post 12 h incubation (scale bar = 10 μm).

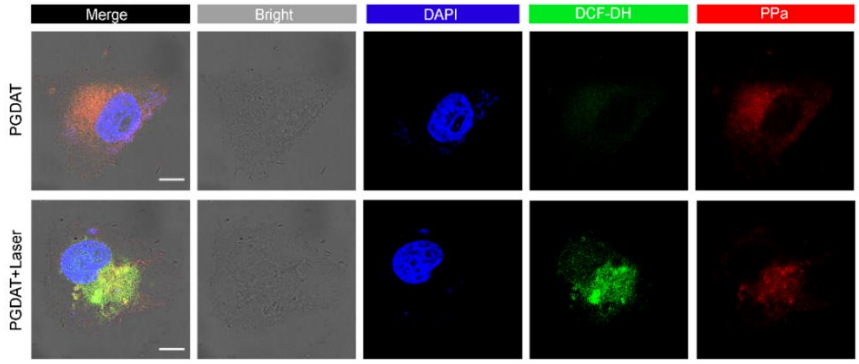

Supplementary Figure 24. CLSM measurement of PDT-mediated ROS generation, the MDA-MB-231 cells were treated with PGDAT nanoparticle for 12 h, and next irradiated with 671 nm laser (scale bar = 10 μm).

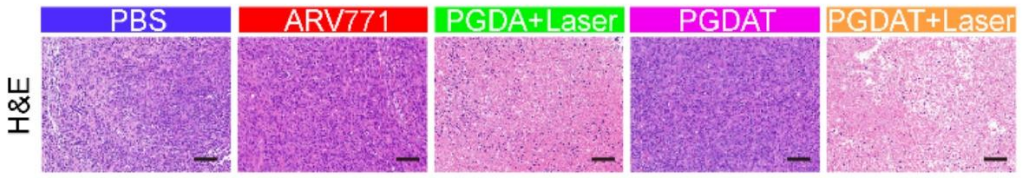

Supplementary Figure 27. H&E staining of the tumor sections at end of treatments (scale bar = 100 μm).

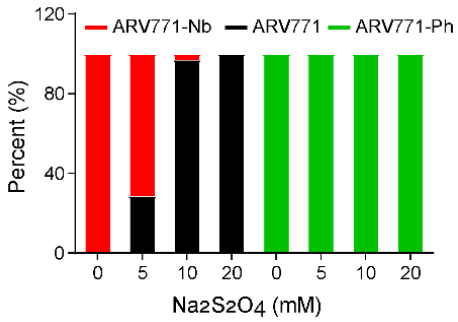

Supplementary Figure 45. Quantitative ARV771 release percentages after ARV771-Nb and ARV771-Ph treated with different concentrations of $Na_2S_2O_4$ using HPLC analysis.

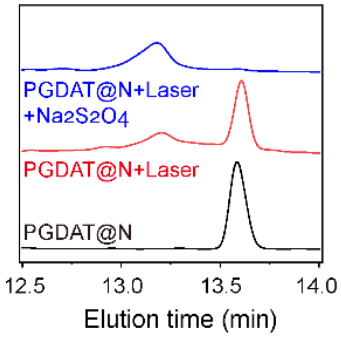

Supplementary Figure 48. HPLC profiles of the photoactivity- and reduction-mediated ARV771

recovery from PGDAT@N nanoparticle

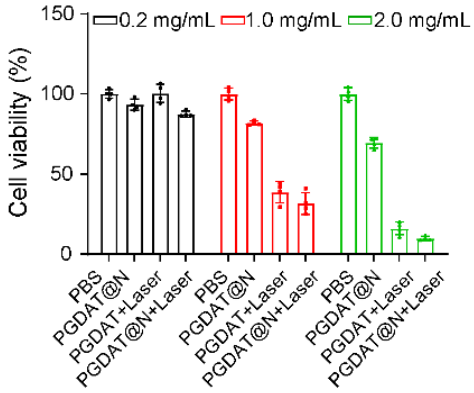

Supplementary Figure 51. CCK-8 analysis of the cell viability of MDA-MB-231 cells 587 treated with diverse patterns (n = 3 biologically independent cells).

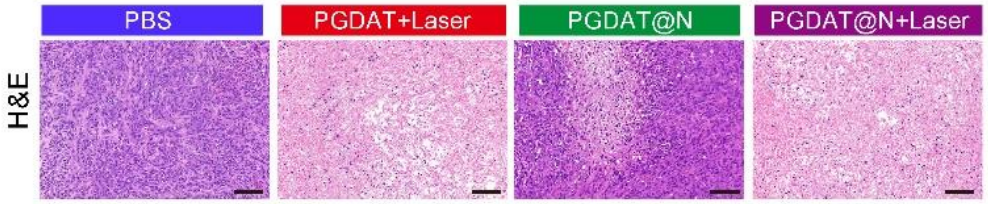

Supplementary Figure 52. H&E staining of the tumor sections at the end of treatments (scale bar = 100 μm).

Reviewer #2 (PROTAC, cancer therapy):

This article by Gao et al describes the development of nanoparticles targeting different cancer cells and responding to different cues to improve their efficiency. The nanoparticles also carry a PROTAC cargo used as a cytotoxic payload. This work aims to overcome some of the limitations of PROTAC molecules, namely pharmacokinetics and to improve tumor specificity. Overall, the manuscript is of decent quality and all the authors' claims are very clearly supported by experiments, to the extent that it almost overwhelms the reader. The amount of work put into this paper is outstanding. This reviewer wonders if all experiments were necessary and if they need to be included in the main text or could be moved to the supporting section. This would allow to highlight the main experiments and streamline the findings. The writing of the manuscript needs some improvement to make the article clearer and give it a better flow. The article would benefit to be made easier to understand. Since the article contains numerous abbreviations and acronyms, it would be good to include in the supporting information a list of all the acronyms/abbreviations used throughout the paper.

Response： To highlight the key points and improve readability of the manuscript, we moved several images from main manuscript to the Supplementary Information, and amplified each image in the whole Figure rationally. Besides, the manuscript was polished by professional editors from Nature Research Editing with the editing certificate was included at the end of this response letter.

According to the suggestion of the reviewer, we added a list of all the acronyms/abbreviations **in Supplementary Table 1**. We also added a cartoon illustration of the nanoparticles prepared in this study in **Supplementary Figure 21** of the revised manuscript.

Supplementary Table 1. List of abbreviations

Abbreviation	Full name
ABL1	abelson murine leukemia viral oncogene homolog 1
BRD4	bromodomain and extraterminal protein 4
CDK1	cyclin-dependent kinase 1
CDK4	cyclin-dependent kinase 4

CDK6	cyclin-dependent kinase 6
CDK7	cyclin-dependent kinase 7
CLSM	confocal laser scanning microscopy
CY	hemicyanine
CSCs	cancer stem-like cells
DEGs	differentially expressed genes
DLS	dynamic light scattering
DPA	2-(diisopropylamino)ethyl methacrylate
GPC	gel permeability chromatography
H&E	hematoxylin and eosin stain
HEMA	2-hydroxyethyl methacrylate
HNSCC	head-neck squamous cell carcinoma
HIF	hypoxia inducible factor
HPLC	high-performance liquid chromatography
^{1}H-NMR	proton nuclear magnetic resonance
KEGG	kyoto encyclopedia of genes and genomes
KLF4	kruppel like factor 4
KRAS	kirsten rat sarcoma viral oncogene
LC-MS	liquid chromatography-mass spectrometry
MDM2	murine double minute 2
MET	c-Mesenchymal-epithelial transition factor
MMP-2	matrix metalloproteinase 2
MS	mass spectrometry
Oct4	octamer-binding transcription factor
p21/CDKN1A	cyclin-dependent kinase inhibitor 1A
PAI	photoacoustic imaging
PDT	photodynamic therapy
PDI	polydispersity index
PEG	poly(ethylene glycol)
POI	protein of interest
PROTAC	PROteolysis TArgeting Chimeras
PPa	pyropheophorbide a
qPCR	quantitative polymerase chain reaction
RAF1	murine leukemia viral oncogene homolog 1
RAFT	reversible addition fragmentation chain transfer
ROS	reactive oxygen species
SOX2	SRY-box transcription factor 2
SOX4	SRY-box transcription factor 4

TEM	transmission electron microscopy
TK	thioketal
TNBC	triple negative breast cancer
TNF	tumor necrosis factor
TUNEL	TdT-mediated dUTP nick end labeling
VHL	Von Hippel-Lindau disease
WNT 7B	wingless-type MMTV integration site family member 7B

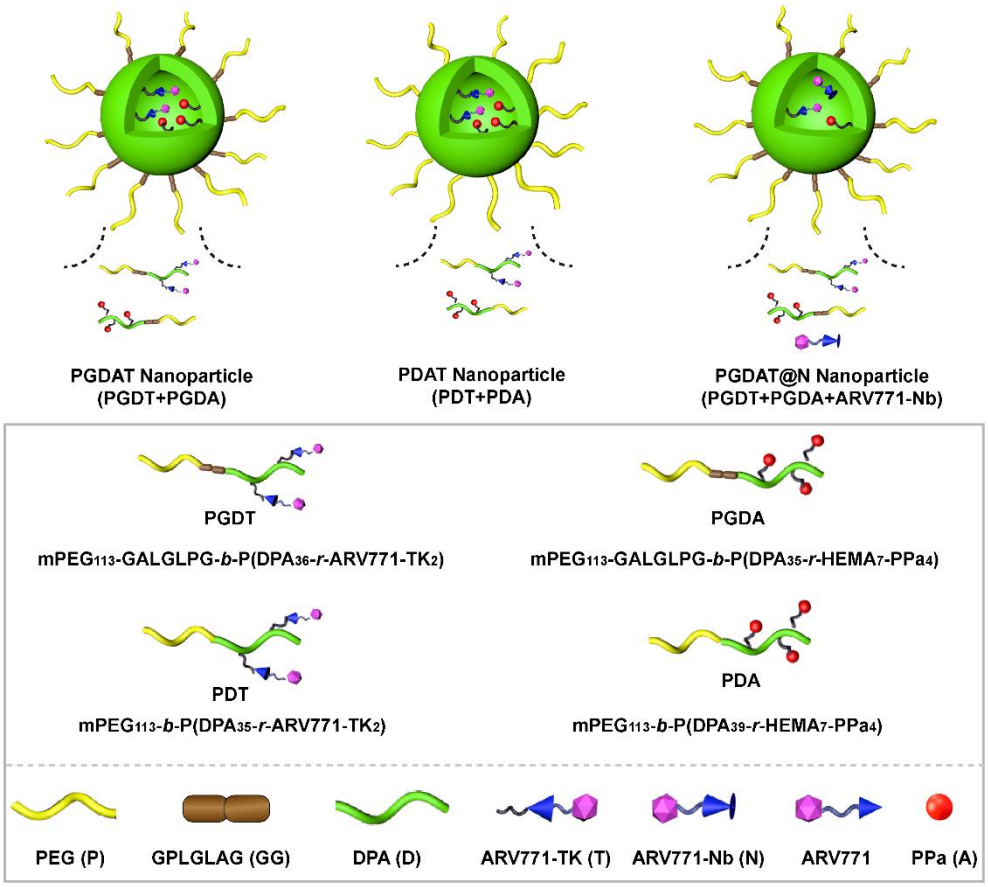

Supplementary Figure 21. Carton illustration of nanoparticle compositions and acronyms investigated throughout our study.

2. In this paper, the authors develop a nanoparticle platform responsive to different extra or intracellular stimuli. Tumor specific accumulation is achieved by using an MMP2 cleavable linker, leading to dePEGylation of the nanoparticles, their cellular uptake and breakdown in the acidic endosomal environment. In addition, the PROTAC payload is cleaved from the polymer by reactive oxygen species generated by laser irradiation of

a photosensitizer. To specifically target stem-like cancer cells, the authors synthesized a redox sensitive PROTAC prodrug. The association of all these technologies creates a very complex platform that the authors characterize very well, from the size of the nanoparticles to the release of the PROTAC in response to different cues. Using this platform the authors claim to have overcome most of PROTACs limitations. Photodynamic therapy involves light laser irradiation at the tumor site, which involves surgery for some solid tumors. This reviewer wonders if an acid cleavable linker responding to tumor specific uptake would be efficient in both regular and stem-like cancer cells.

Response： We appreciate the constructive comments of the reviewer. It is an elegant idea to utilize acid-cleavable linker to activate the prodrug in both normal and hypoxia tumor cells. We are actually developing acid-liable PROTAC prodrugs, which will be submitted soon.

In this study, to perform region-confined protein degradation in the normoxia and hypoxia tumor cells, we modified the BRD4 PROTAC with ROS- and reduction-activatable protection groups, respectively. The ROS-liable ARV771-TK can be activated to ablate the targeted protein in the normoxia region. In contrast, the hypoxia-responsive ARV771-Nb prodrug can be restored with nitroreductase, and degraded the targeted proteins in the hypoxia tumor lesion. This strategy actually provides a robust tool for spatially-confided regulating protein hemostasis in the tumor mass.

3. Given the amount of work and the care given to characterizing their platform, this paper has the potential to interest the readers of Nature Communications. However, it needs to go through some revisions before being published.

• The grammar and the spelling of the paper and the supporting information needs to be thoroughly checked and modified. As it stands, the paper is too confusing and errors or complex sentences take the attention away from the results. Special attention needs to be brought to the Abstract, the introduction, and the conclusion. This will elevate the quality of the manuscript tremendously and will make it easier to follow. Some examples below:

o Line 46: and penetrate into deep tumor via liable to MMP2. A word seems to be missing.

Response: We appreciate the critical comments of the reviewer. To make the manuscript more readable, we thoroughly polished the English writing of the manuscript, and carefully revised the Abstract, introduction, and the conclusion. Besides, the manuscript was polished by professional editors from Nature Research Editing with the editing certificate was included at the end of this response letter.

The sentence in line 46 was revised as "These PROTAC nanoparticles selectively accumulate within and penetrate deep into tumors via response to matrix metalloproteinase-2."

o Line 67: PROTAC is misspelled

Response: Revised.

o Line 103: we further innovated a hypoxia-responsive PROTAC

Response: We revised this sentence to "we further designed a hypoxia-responsive PROTAC prodrug".

o Line 676: we engineered fashioned a region-confined PROTAC

Response: We revised this sentence to "we fashioned a region-confined PROTAC". Besides, to improve the readability, the manuscript was thoroughly revised by a professional editor from Nature Research Editing group.

4. The PGDAT nanoparticles were synthesized using a ratio of 2/1 PROTAC monomer to photo sensitizer monomer. Did the authors try different ratios of PROTAC/Photosensitizer (PPa)? Was the 2/1 ratio the one giving the best results?

Response: The PROTAC and PPa feeding ratio was determined by their administration doses *in vivo*. In previous studies, we found that PDT with PPa-loaded nanoparticles completely inhibited breast tumor growth as a PPa dose of 5.0 mg/kg[1, 2]. Furthermore, we demonstrated that ARV-771 prodrug suppressed breast tumor growth at a ARV771 dose of 10 mg/kg[3]. Therefore, we prepared the PROTAC prodrug nanoparticles at a consistent PROTAC/PPa weight ratio of 2/1.

[1] Hou B, Zhou L, Wang H, Saeed M, Wang D, Xu Z, Li Y, Yu H. Engineering Stimuli-Activatable

Boolean Logic Prodrug Nanoparticles for Combination Cancer Immunotherapy. Adv Mater. 2020, 32(12): e1907210.

[2] Gao A, Chen B, Gao J, Zhou F, Saeed M, Hou B, Li Y, Yu H. Sheddable Prodrug Vesicles Combating Adaptive Immune Resistance for Improved Photodynamic Immunotherapy of Cancer. Nano Lett. 2020, 8; 20(1): 353-362.

[3] Zhang S, Lai Y, Pan J, Saeed M, Li S, Zhou H, Jiang X, Gao J, Zhu Y, Yu H, Zhang W, Xu Z. PROTAC Prodrug-Integrated Nanosensitizer for Potentiating Radiation Therapy of Cancer. Adv Mater. 2024, 14: e2314132.

5. Figure 2c. and figure 2e. The BRD4 levels in figure 2c appear much higher than in figure 2e, or at least the corresponding band on the western blot appears more important. Is this due to overexposure to try to really highlight the degradation of BRD4 at 500 nM ARV771? Or is the level of BRD4 lower in the cells treated with ARV771-TK?

Response: The BRD4 level in Figure 2c looks higher than that Figure 2e, which is caused by extended exposure time due to largely reduced BRD4 expression upon PROTAC treatment. To avoid misunderstanding, we updated the contrast of Figure 2c to make BRD4 level to be comparable to Figure 2e.

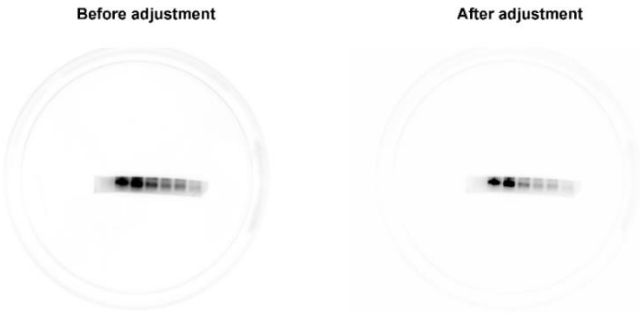

Figure 1 (for reviewer only): The uncropped images of Figure 2c before and after adjustment.

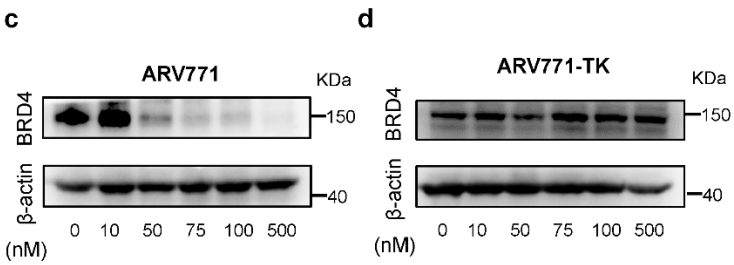

Figure 2c&d: Western blot images of ARV771/ARV771-TK-mediated BRD4 degradation in MDA-MB-231 cells post 24 h of co-incubation.

6. Figure 3b/e + 8c. the microscopy images are hard to read in printed version and sometimes still very hard to read on a computer screen. It is extremely unclear to an untrained eye to see major differences. These figures would benefit from being moved to the supporting information and being much larger. For all the cell imaging, it would be interesting to add in the supporting information a phase contrast image of the cells.

Response： As suggested by the reviewer, we moved Figure 3b/e to the Supplementary Information as Supplementary Figure 23 and Supplementary Figure 24, and magnified the images to enhance the clarity of details. We also added the phase contrast image in Supplementary Figure 23 and Supplementary Figure 24.

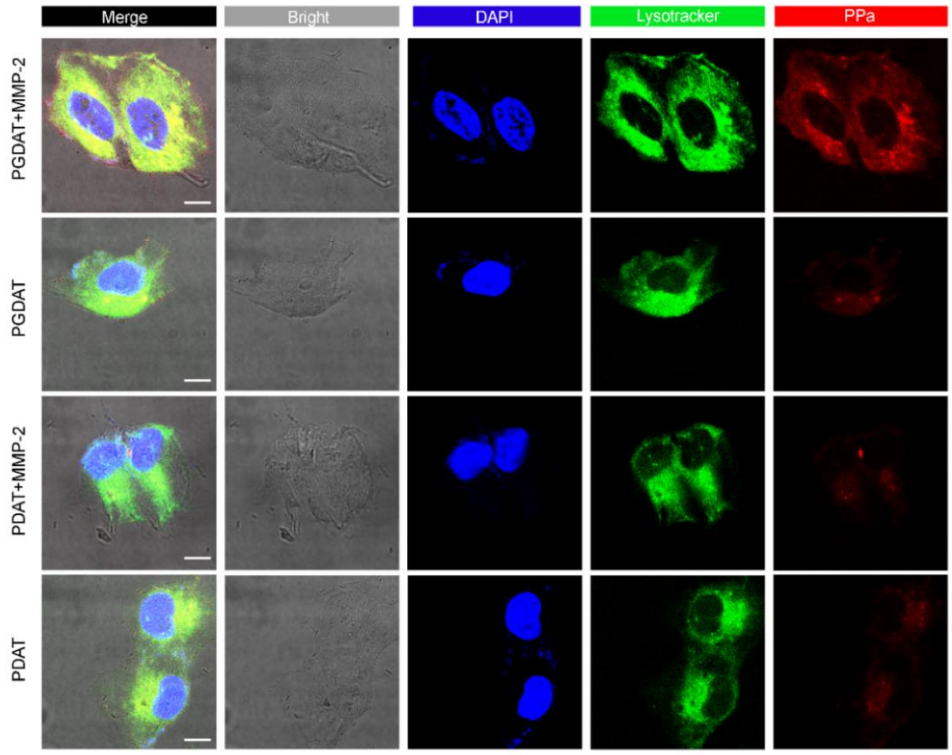

Supplementary Figure 23. Representative CLSM images of the intracellular distribution of the PROTAC nanoparticle post 12 h incubation (scale bar = 10 μm).

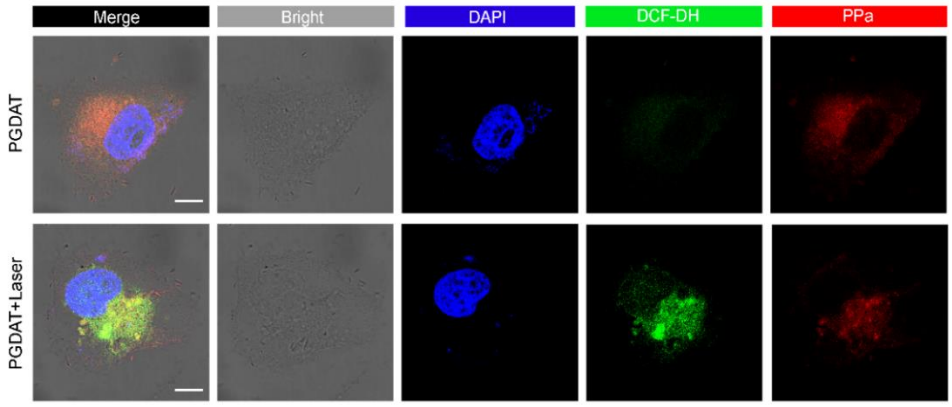

Supplementary Figure 24. CLSM measurement of PDT-mediated ROS generation, the MDA-MB-231 cells were treated with PGDAT nanoparticle for 12 h, and next irradiated with 671 nm laser (scale bar = 10 μm).

Furthermore, to improve the quality of the CLSM images, we re-defined CY as red and pimo as green in Figure 8c (Figure 7c in the revised manuscript), and added the semi-quantitation data in **Supplementary Figure 68** of the revised manuscript.

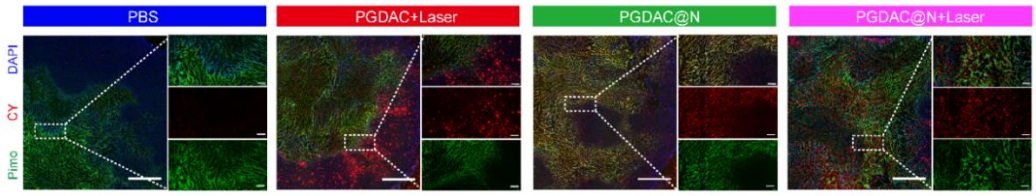

Figure 7c. Ex-vivo CLSM images of the tumor sections post treatments for analysis of hypoxia (pimonidazole, pimo) and CY fluorescence (left panel scale bar = 1.0 mm, right panel scale bar = 200 μm, the right images from top to bottom represent Merge, CY and Pimo respectively).

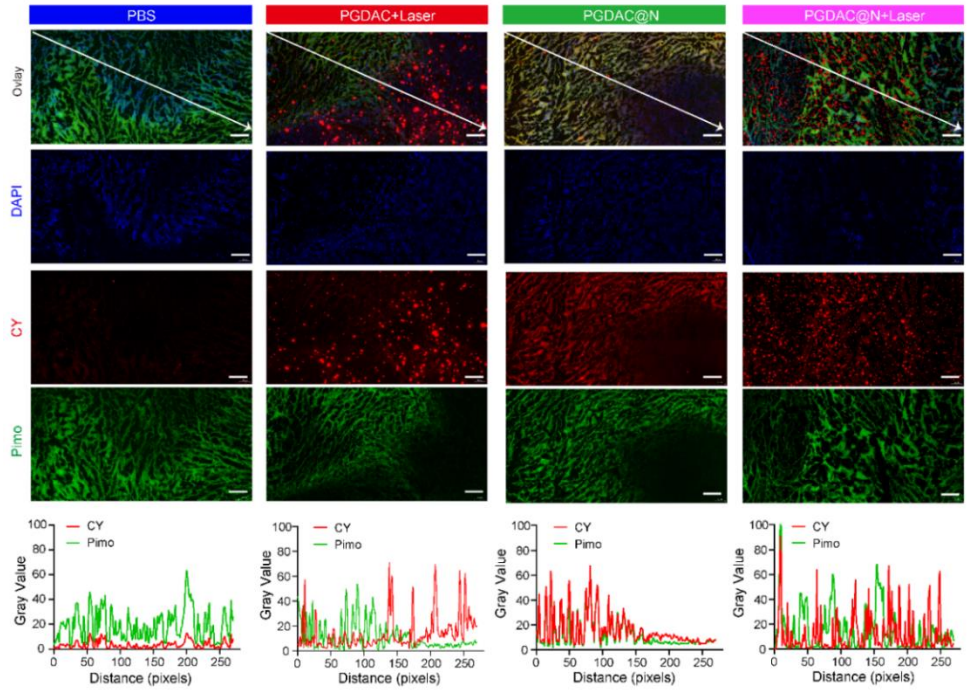

Supplementary Figure 68. Ex-vivo CLSM images of tumor section post subjected to different treatments (scale bar = 200 μm) and the gray value as the arrow indicated area.

7. Figure 3e. Was the cytotoxicity of the irradiation tested? Would that be a concern?

Response: The PROTAC nanoparticles displayed negligible phototoxicity at a concentration below 0.2 mg/mL (Figure 3h in the original manuscript, which is renumbered as Figure 2n in the revised manuscript). We selected PGDAT nanoparticle concentration of 0.13 mg/mL (PPa concentration of 10 μM) for investigating ROS generation *in vitro*. Therefore, the interference of irradiation-induced cytotoxicity was ruled out.

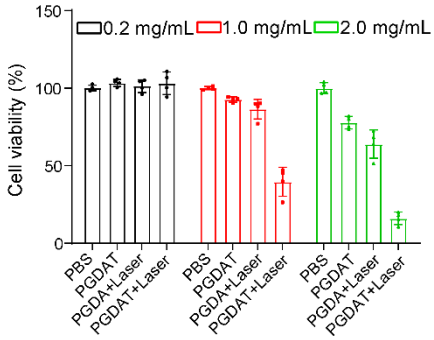

Figure 2n. CCK-8 assay of MDA-MB-231 cell viability post different treatments (n = 3 biologically independent cells).

8. Figure 8a: Levels of HIF also appear much weaker with PGDAT@N than for other nanoparticles or the PBS control. Is HIF expression or stability being impacted by PGDAT@N?

Response: Actually, experimental groups with laser irradiation displayed slightly higher HIF expression in the tumor sections, and the treated with PGDAT@N nanoparticle displayed comparable HIF expression in the tumor sections with PBS treated group. To make the immunofluorescence staining images more visible, we amplified Figure 8a (Figure 7a in the revised manuscript) and semi-quantified the fluorescence value of each image (Supplementary Figure 57 in the revised manuscript).

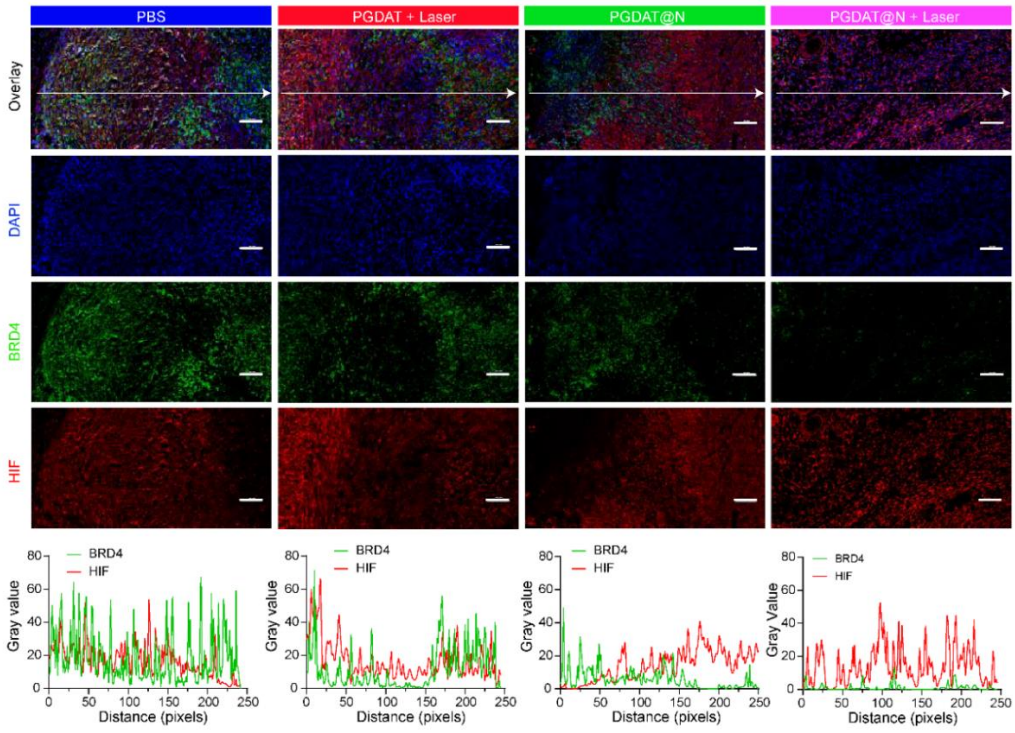

Supplementary Figure 57. Ex-vivo CLSM images of the tumor section post to different treatments (scale bar = 200 μm), with the semi-quantified fluorescence value of the arrow indicated area included.

9. Figure 8c. The overlay between the two colors used for pimo and Cyanine are extremely hard to tell apart. It would be good to mention in the caption what each smaller zoomed in section corresponds to. I suppose, the top one is an overlay while the two bottom ones correspond respectively to Pimo and Cy.

Response: To improve discrimination, we possessed CY as red and pimo as green in

Figure 8c (Figure 7c in the revised manuscript), and added annotation of each image in the Figure legend.

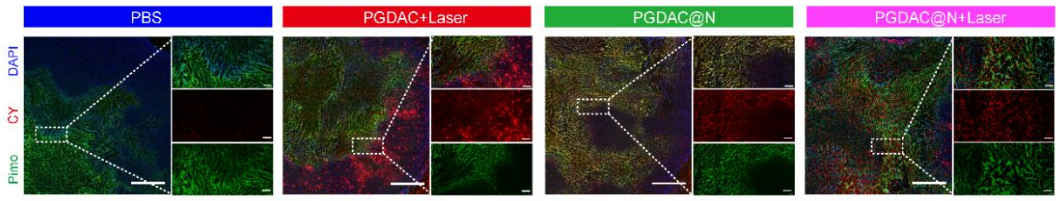

Figure 7c. Ex-vivo CLSM images of tumor sections post tumor-bearing mice subjected to various treatments for analysis of hypoxia (pimonidazole, Pimo) and CY fluorescence (left panel scale bar = 1.0 mm, right panel scale bar = 200 μm, the right images from top to bottom represent Merge, CY and Pimo respectively).

10. In general, comparing the in vivo efficacy of PDGAT versus PDGAT@N. What would be the impact of restarting the treatment with PDGAT for the mice that relapsed? Do the authors expect PDGAT@N to still outperform PDGAT? I understand that performing this experiment would be asking a lot and would not necessarily add much to the paper. This is more sheer curiosity.

Response: We appreciate the reviewer for the insightful comments and suggestions. This is a very critical question to check whether the PROTAC nanoparticles could inhibit reoccurred tumor post treatment. Honestly, we did not check the profile of the PROTAC nanoparticles for treatment of the relapsed tumors. However, as shown in Figure 6i and Figure 7f of the revised manuscript, the combination of PDT and PGDAT@N performed much better than PGDAT + laser to inhibit primary tumor growth due to their (PGDAT@N + laser) ability to eradicate both normoxic and hypoxic tumor cells. It has been reported that stem-like tumor tumors play a key role in tumor relapse and distance metastasis. Therefore, we would predict better anti-tumor performance of PGDAT@N + laser compared to PGDAT + laser in the relapsed tumor models, which will be investigated in future studies.

11. Supplementary figure 25: Title of the caption needs to be changed to Heat map.

Response: Corrected.

12. Supplementary figure 51 + 52: The overall quality of the analysis of compound 32 is very poor. The resolution of the NMR spectrum does not allow for a good assignment of the signals. The MS spectrum needs to be shown in full and not zoomed in. This mas spectrum cannot be used to interpret the purity of this compound. The characterization of this compound needs to be brought to the same level of detail as the previous compounds in this paper.

Response: We updated the ^{1}H-NMR and mass spectrum of compound 32 in Supplementary Figure 61&62 of the revised manuscript.

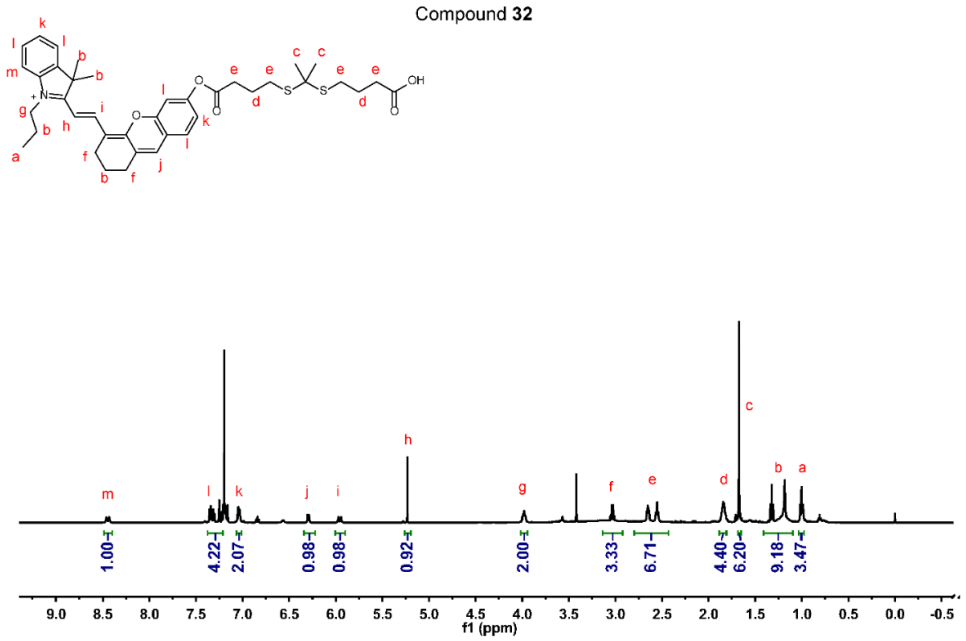

Supplementary Figure 61. ^{1}H-NMR spectrum of compound **32** ($CDCl_3$).

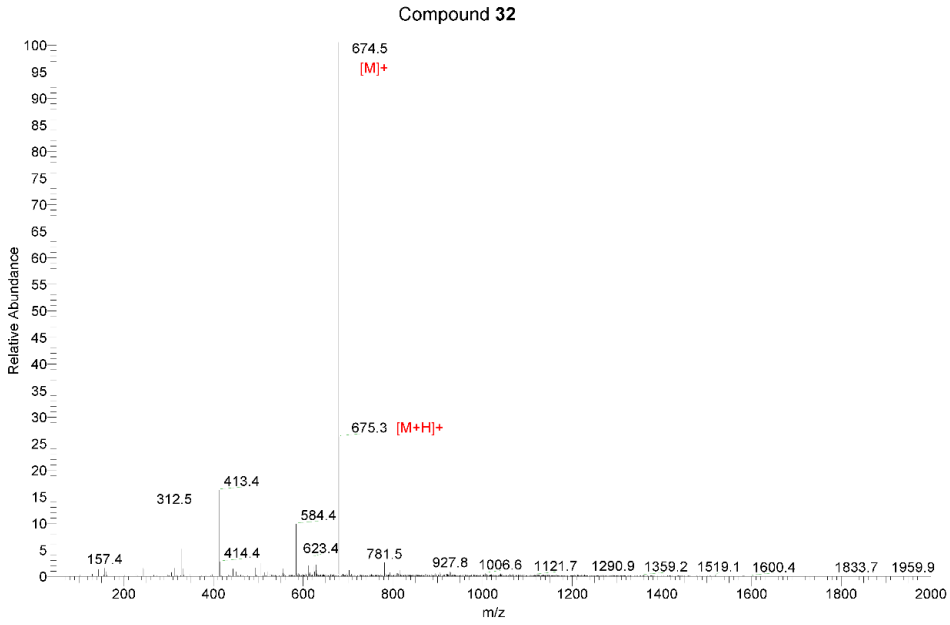

Supplementary Figure 62. Mass spectrum of compound **32** ($CDCl_3$).

Reviewer #3 (CSC, cancer therapy):

Gao and coauthors are dealing with an important problem of targeting tumor heterogeneity using PROTAC-based treatment. The authors proposed an elegant design of the BRD4-specific, ROS- and hypoxia-activated PROTAC nanoplatform. Overall, this interesting and comprehensive study can undoubtedly be of interest to the interdisciplinary scientific community. The results shown in this manuscript are novel and pertinent. Still, some issues must be clarified.

Main concerns:

1. Clinical relevance:

- The activation of the PROTAC system is pH dependent and is responsive to low intracellular acidity (pH 5.5-6.5). However, some tumor types upregulate expression of Na+/H+ exchanger 9 (NHE9) associated with more alkaline endosomes (pH > 6.5), stemness, and worse clinical outcome (e.g., Kondapalli et al., Nat. Commun. 2015; Ko et al., PNAS Nexus 2022). NHE9 is upregulated in different malignancies, and its high expression is related to poor prognosis (e.g., in CRC and ESCC).

Response: Exactly, tumor heterogenicity could be a major concern for clinical cancer therapy. As mentioned by the reviewer, Rao and co-workers found that NHE9 is overexpressed in some subtypes of glioblastoma, for example GBM612. NHE9 as the endosomal Na+/H+ exchanger, is mainly expressed in early and recycling endosomes. The elevated NHE9 expression may alkylate the endosomal lumen up to pH 6.90 ± 0.47 as measured by a ratiometric method. However, an acidic microenvironment is predicted in the late endosome and lysosome where without NHE9 expression according to the literature reports[1-3]. On the other hand, it was reported that NHE9 is overactivated in a subtype of glioblastoma tumors, other types of glioblastoma tumors (e.g., GMB 253 and GMB 276 tumor) display normal or reduced NHE9 expression patterns. The GMB 276 tumor with low NHE9 level still show acidic endosomal pH of 5.57±0.13[4, 5].

In this study, we developed a PROTAC nanoparticle by integrating acid-responsive polymer backbone, and radical oxygen species- and hypoxia-liable PROTAC prodrugs into one single nanoplatform. The PROTAC nanoparticles therefore can respond to

acidic endo/lysosomal environment (pH < 6.3) to expose/release the PROTAC prodrugs, and subsequently restore the BRD4 PROTAC either in normal tumor cells (triggered by PDT) or in CSCs (activated by nitroreductase). To demonstrate the potential the PROTAC nanoparticles, we selected triple negative breast cancer and head neck carcinoma tumor models sine PDT of these two kinds of tumors had been clinically investigated. Taken together, we consider that NHE9-induced pH up-regulation in the early endosome of glioblastoma subtypes will not compromise the anti-tumor efficacy of the acid-responsive nanoplatform presented in this manuscript.

[1] Wang Y, Zhou K, Huang G, Hensley C, Huang X, Ma X, Zhao T, Sumer BD, DeBerardinis RJ, Gao J. A nanoparticle-based strategy for the imaging of a broad range of tumours by nonlinear amplification of microenvironment signals. Nat Mater. 2014 Feb;13(2):204-212.

[2] Casey, J. R., Grinstein, S. & Orlowski, J. Sensors and regulators of intracellular pH. Nat. Rev. Mol. Cell Biol. 11, 50–61 (2010)

[3] Chen B, Yan Y, Yang Y, Cao G, Wang X, Wang Y, Wan F, Yin Q, Wang Z, Li Y, Wang L, Xu B, You F, Zhang Q, Wang Y. A pyroptosis nanotuner for cancer therapy. Nat Nanotechnol. 2022 Jul;17(7):788-798.

[4] Kondapalli KC, Llongueras JP, Capilla-González V, Prasad H, Hack A, Smith C, Guerrero-Cázares H, Quiñones-Hinojosa A, Rao R. A leak pathway for luminal protons in endosomes drives oncogenic signalling in glioblastoma. Nat Commun. 2015 Feb 9; 6:6289.

[5] Ko M, Makena MR, Schiapparelli P, Suarez-Meade P, Mekile AX, Lal B, Lopez-Bertoni H, Kozielski KL, Green JJ, Laterra J, Quiñones-Hinojosa A, Rao R. The endosomal pH regulator NHE9 is a driver of stemness in glioblastoma. PNAS Nexus. 2022 Mar 9;1(1): pgac013.

2. Next, the problem with targeting BRD4 could be associated with potential target escape due to tumor cell plasticity and heterogeneity, including CSCs. One suggested approach could be a dual/multiple targeting, leading to a synergistic effect and preventing tumor cell escape.

Response: We completely agree with reviewer that single target therapy has the risk of target escape due to tumor cell plasticity and heterogeneity.

In this work, we selected BRD4 as a target to demonstrate the potential of our two-

in-one PROTAC prodrug nanoplatform for region-confined protein degradation and breast cancer therapy. BRD4 is a transcriptional and epigenetic regulator, which is extensively investigated for cancer therapy. Inhibition of BRD4 pathway can suppress proliferation and induce apoptosis of tumor cells. Clinical trials have validated that BRD4 inhibition is effective for treatment of some human cancers, including multiple myeloma, acute myelogenous leukemia, breast cancer and so on[1-3]. Furthermore, it was reported that BRD4 inhibition could eradicate cancer stem-like cells by downregulating CDK4/6 pathway and inducing apoptosis of CSCs[4-6]. Therefore, for proof-of-concept, we selected BRD4 as the protein target to demonstrate the potential of the region-confined PROTAC nanoparticles for spatially-tunable protein degradation and cancer therapy.

Of note, to avoid tumor relapse due to tumor plasticity and heterogeneity, we will try to integrate dual/multiple targeting into one system for overcoming tumor heterogeneity, which will be investigated in future study.

[1] Bai L, Zhou B, Yang CY, Ji J, McEachern D, Przybranowski S, Jiang H, Hu J, Xu F, Zhao Y, Liu L, Fernandez-Salas E, Xu J, Dou Y, Wen B, Sun D, Meagher J, Stuckey J, Hayes DF, Li S, Ellis MJ, Wang S. Targeted Degradation of BET Proteins in Triple-Negative Breast Cancer. Cancer Res. 2017 May 1;77(9):2476-2487.

[2] Donati B, Lorenzini E, Ciarrocchi A. BRD4 and Cancer: going beyond transcriptional regulation. Mol Cancer. 2018 Nov 22;17(1):164.

[3] Shi J, Wang Y, Zeng L, Wu Y, Deng J, Zhang Q, Lin Y, Li J, Kang T, Tao M, Rusinova E, Zhang G, Wang C, Zhu H, Yao J, Zeng YX, Evers BM, Zhou MM, Zhou BP. Disrupting the interaction of BRD4 with diacetylated Twist suppresses tumorigenesis in basal-like breast cancer. Cancer Cell. 2014 Feb 10;25(2):210-225.

[4] Di Micco R, Fontanals-Cirera B, Low V, Ntziachristos P, Yuen SK, Lovell CD, Dolgalev I, Yonekubo Y, Zhang G, Rusinova E, Gerona-Navarro G, Cañamero M, Ohlmeyer M, Aifantis I, Zhou MM, Tsirigos A, Hernando E. Control of embryonic stem cell identity by BRD4-dependent transcriptional elongation of super-enhancer-associated pluripotency genes. Cell Rep. 2014 Oct 9;9(1):234-247.

[5] Dong J, Li J, Li Y, Ma Z, Yu Y, Wang CY. Transcriptional super-enhancers control cancer

stemness and metastasis genes in squamous cell carcinoma. Nat Commun. 2021 Jun 25;12(1):3974.

[6] Yang A, Qin S, Schulte BA, Ethier SP, Tew KD, Wang GY. MYC Inhibition Depletes Cancer Stem-like Cells in Triple-Negative Breast Cancer. Cancer Res. 2017 Dec 1;77(23):6641-6650

3. Next, the tissue penetration depth of the laser irradiation is limited to a few mm, sufficient to see a therapeutic effect in subcutaneous tumor models but not for orthotopic tumors/in a clinical setting Together, these considerations raise concern about the possible clinical applicability of the suggested PROTAC nanoplatforms.

Response: Exactly, limited tissue penetration depth could be one of the major concerns for phototherapy of the orthotropic tumors in the major organs (e.g., liver and brain). Therefore, we selected orthotropic breast tumor model to demonstrate the potential of the PROTAC nanoparticles for breast cancer therapy. Furthermore, with the emerging advances of fiber optics and other interventional techniques, the laser photo source can be guided deep into the body, thus enforce the translation potential of cancer phototherapy. Furthermore, we are also exploiting the potential of other kinds of external stimulus including ultrasonication and ion radiation with deep tissue penetration ability to restore the PROTAC prodrug *in vivo*. There strategies could largely improve the clinical applicability of the PROTAC nanoplatforms

We added above discussion in page 37 of the revised manuscript.

4. In vivo models:

- The authors described MDA-MB-231 and HN30 orthotopic murine models in the material and methods; however, the results included in the figures were obtained only with subcutaneous models. Validation of the therapeutic effect in the orthotropic models would increase the translational potential of the described nano platform. The authors are encouraged to include these models in the revised study.

Response: An orthotopic MDA-MB-231 breast tumor model and a subcutaneously implanted HN30 head and neck tumor model were used for the anti-tumor study. To construct the orthotopic breast tumor model, MDA-MB-231 tumor cells were injected

into the second mammary fat pad of nude mouse, which could mimic the actual growth environment of breast cancer as reported in the literatures (Figure 3)[1, 2]. However, it is difficult to establish and monitor the orthotopic head and neck (HNSCC) tumor model since the tumor implanted at the base of tongue could affect the physiological activity of the experimental mice. We will try our best to investigate the antitumor performance of the prodrug nanoparticles in more orthotropic tumor models in future investigation.

We revised the description in the method section of the manuscript.

Figure 2 (for reviewer only): Photographs for orthotropic breast tumor inoculation by injecting MDA-MB-231 tumor cells into the second mammary fat pad of nude mouse.

[1] Paschall AV, Liu K. An Orthotopic Mouse Model of Spontaneous Breast Cancer Metastasis. J Vis Exp. 2016 Aug 14;(114):54040.

[2] Ouyang J, Sun L, Zeng Z, Zeng C, Zeng F, Wu S. Nanoaggregate Probe for Breast Cancer Metastasis through Multispectral Optoacoustic Tomography and Aggregation-Induced NIR-I/II Fluorescence Imaging. Angew Chem Int Ed Engl. 2020 Jun 15;59(25):10111-10121.

5. The group size (n = 6) and partially overlapping tumor growth curves (e.g., for PGDA+Laser vs. PGDAT+Laser in Figure 5D) raise a concern about statistical analysis, giving p = 0.0084 for the mentioned groups. The authors should clarify the statistical

method in the legends of Figure 5.

Response: We appreciate the kind reminder of the reviewer. The p value between PGDA + laser and PGDAT + laser groups was recalculated to be 0.0461. We also added the statistical methods in the Figure legends of the revised manuscript.

6. Other concerns:

- Figure 5-7: how is it possible that PGDAT + Laser treatment leads to an increase in the hypoxic area and CSC populations?

Response: Exactly, PGDAT + laser treatment slightly increased the hypoxic area and CSC populations since PDT can consume oxygen and induces hypoxia condition in the tumor tissue. The hypoxia tumor microenvironment would facilitate proliferation of cancer stem-like cell as reported previously[33-36]. Notably, PDT-induced elevation of CSC population could be eradicated by the hypoxia-activatable PROTAC prodrug ARV771-Nb. We added above discussion in page 4, 21 and 22 of the revised manuscript.

[33] Diehn M, Cho RW, Lobo NA, Kalisky T, Dorie MJ, Kulp AN, Qian D, Lam JS, Ailles LE, Wong M, Joshua B, Kaplan MJ, Wapnir I, Dirbas FM, Somlo G, Garberoglio C, Paz B, Shen J, Lau SK, Quake SR, Brown JM, Weissman IL, Clarke MF. Association of reactive oxygen species levels and radioresistance in cancer stem cells. Nature. 2009 Apr 9;458(7239):780-783.

[34] Zhang J, Li L. Stem cell niche: microenvironment and beyond. J Biol Chem. 2008 Apr 11;283(15):9499-9503.

[35] Li Z, Rich JN. Hypoxia and hypoxia inducible factors in cancer stem cell maintenance. Curr Top Microbiol Immunol. 2010; 345:21-30.

[36] Kim JH, Verwilst P, Won M, Lee J, Sessler JL, Han J, Kim JS. A Small Molecule Strategy for Targeting Cancer Stem Cells in Hypoxic Microenvironments and Preventing Tumorigenesis. J Am Chem Soc. 2021 Sep 8;143(35):14115-14124.

7. Although the authors conclude that BRD4 degradation influences the CSC population, the evidence from in vivo experiments e.g., analysis of the CSC populations in the experimental treated tumors, did not confirm this statement. The results of the flow cytometry examination of CD44+/CD24- cells did not show a statistically significant

difference between control PBS-treated and PGDAT@N + Laser treated mice.

Response: We appreciate the critical comments of the reviewer. Actually, there is statistically significant difference between the cancer stem-like cells ratios of PBS and PGDAT@N + laser groups when the re-analyzed the flow cytometry data. The statistic data was included in Figure 6o of the revised manuscript.

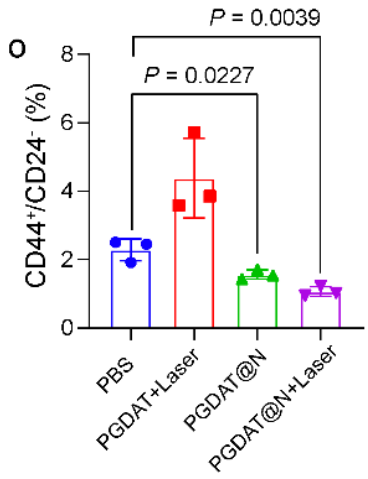

Figure 6o. Flow cytometry examination of CSCs ratio in the tumor tissue post treatments (n = 3 biologically independent mice). Statistical analysis was performed by two-side unpaired t-test.

REVIEWERS' COMMENTS

Reviewer #1 (Remarks to the Author):

The revised manuscript has addressed most of the reviewers' comments and criticisms in a satisfactory manner, and I now consider it suitable for publication in Nature Communications.

Reviewer #2 (Remarks to the Author):

Based on the changes made by the authors and the answers given to all the reviewers concerns, I support the publication of this manuscript in its current form.

Reviewer #3 (Remarks to the Author):

The authors satisfactorily addressed the reviewers' critique in the revised version of the manuscript. I have no further comments.